Identification of a Thyroid Hormone Response Element in the Mouse Krüppel-Like Factor 9 Gene to Explain Its Postnatal Expression in the Brain

Robert J. Denver and Keith E. Williamson

Department of Molecular, Cellular, and Developmental Biology, The University of Michigan, Ann Arbor, Michigan 48109-1048

Brain development is critically dependent on thyroid hormone (T_3). Krüppel-like factor 9 (*Klf9*) is a T_3-inducible gene in developing rat brain, and several lines of evidence support that KLF9 plays a key role in neuronal morphogenesis. Here we extend our findings to the mouse and demonstrate the presence of a functional T_3 response element (T_3RE) in the 5′ flanking region of the mouse *Klf9* gene. *Klf9* mRNA is strongly induced in the mouse hippocampus and cerebellum in a developmental stage- and T_3-dependent manner. Computer analysis identified a near optimal direct repeat 4 (DR-4) T_3RE 3.8 kb upstream of the *Klf9* transcription start site, and EMSAs showed that T_3 receptor (TR)-retinoid X receptor heterodimers bound to the T_3RE with high affinity. The T_3RE acts as a strong positive response element in transfection assays using a minimal heterologous promoter. In the mouse neuroblastoma cell line N2a[TRβ1], T_3 caused a dose-dependent up-regulation of *Klf9* mRNA. Chromatin immunoprecipitation assays conducted with N2a[TRβ1] cells showed that TRs associated with the *Klf9* T_3RE, and this association was promoted by T_3. Treatment of N2a[TRβ1] cells with T_3 led to hyperacetylation of histones 3 and 4 at the T_3RE site. Furthermore, TRs associated with the DR-4 T_3RE in postnatal d 4 mouse brain, and histone 4 acetylation was greater at this site compared with other regions of the *Klf9* gene. Our study identifies a functional DR-4 T_3RE located in the mouse *Klf9* gene to explain its regulation by T_3 during mammalian brain development. **(*Endocrinology* 150: 3935–3943, 2009)**

Thyroid hormone deficiency during the period of active neurogenesis (up to 6 months postpartum) results in irreversible mental retardation (*i.e.* cretinism) that is associated with multiple morphological alterations in the brain (1, 2). Thyroid hormone exerts pleiotropic actions on the developing brain, influencing diverse processes such as neuronal maturation, neurite outgrowth, synapse formation, cell proliferation, timing of cell differentiation, and myelination (2). Hypothyroidism during fetal and neonatal life results in abnormal axonal development and greatly reduced dendritic arborization in specific cell populations (3–7). Krüppel-like factor 9 (*Klf9*; also basic transcription element binding protein 1) (8), a member of the specificity protein/Krüppel-like family of zinc-finger domain transcription factors (9, 10), is strongly induced by T_3 in the developing brain of frog (11, 12) and rat (13). KLF9 plays a key role in thyroid hormone-dependent actions on neurite extension and branching (13–15), and Morita *et al.* (16) showed that disruption of the mouse *Klf9* locus resulted in reduced dendritic arborization in cerebellar Purkinje cells and behavioral deficits consistent with abnormal functions of the amygdala, hippocampus, and cerebellum.

Several lines of evidence suggest that *Klf9* is a direct thyroid hormone response gene. For example, T_3 induction of *Klf9* in the mouse-derived neuroblastoma cell line N2a[TRβ1] (17) is resistant to protein synthesis inhibition, and nuclear run-on analysis showed that T_3 increased the rate of *Klf9* transcription (13). The immediate early kinetics of *Klf9* gene regulation in mammalian and frog cells supports direct transactivation by liganded thyroid hormone receptor (TR) (13, 18, 19). These actions are likely mediated by one or more thyroid hormone response elements (T_3REs) present in the *Klf9* gene. Furlow and Kanamori (18) demonstrated the presence of a direct repeat 4 (DR-4) T_3RE in the *Xenopus laevis Klf9* 5′ flanking region.

ISSN Print 0013-7227 ISSN Online 1945-7170
Printed in U.S.A.

doi: 10.1210/en.2009-0050 Received January 14, 2009. Accepted March 31, 2009.
First Published Online April 9, 2009

Abbreviations: acH3, Acetylated histone 3; acH4, acetylated histone 4; ChIP, chromatin immunoprecipitation; DR-4, direct repeat 4; DPBS, Dulbecco's PBS; DSP, dithiobis[succinimidyl propionate]; GAPDH, glyceraldehyde-3-phosphate dehydrogenase; IP, inverted palindrome; KLF9, Krüppel-like factor 9; NRS, normal rabbit serum; NSB, nonspecific binding; P, postnatal day; RXR, retinoid X receptor; TR, thyroid hormone receptor; T_3RE, T_3 response element.

In the present study, we investigated the molecular basis for T_3 regulation of the *Klf9* gene in developing mouse brain. We first confirmed that *Klf9* is developmentally regulated and induced by T_3 in the mouse brain as we earlier found it to be in the rat (13). We next analyzed the mouse *Klf9* gene and its 5′ flanking region for the presence of putative T_3REs. We identified a near optimal DR-4 T_3RE located about 3.8 kb upstream of the transcription start site. Using EMSA, *in vitro* transfection assay and chromatin immunoprecipitation (ChIP) assay, we tested whether this DR-4 T_3RE was functional in both cell culture using N2a[TRβ1] cells and neonatal mouse brain *in vivo*.

Materials and Methods

Animals

Wild-type C57BL/6j mice were purchased from Jackson Laboratories (Bar Harbor, ME) and bred in the laboratory. Animals were euthanized and brain tissue harvested at different postnatal days for gene expression analyses. For gene expression analyses and ChIP assays neonatal mice [postnatal day (P) 4] were given ip injections of saline or 3,5,3′ triiodothyronine (T_3 sodium salt; 25 μg/kg body weight; Sigma, St. Louis MO), euthanized 4 h later, and blood plasma and brain tissue harvested for analysis. All procedures were conducted in accordance with guidelines of The University of Michigan Committee on the Care and Use of Animals.

RNA isolation and gene expression analysis by quantitative, real-time RT-PCR

We extracted RNA from microdissected mouse brain sections that contained either the hippocampus or cerebellum or from N2a[TRβ1] cells using the Trizol reagent (Invitrogen, Carlsbad, CA) following the manufacturer's instructions. The RNA was treated with deoxyribonuclease I and ribonuclease inhibitor before cDNA synthesis with Superscript II (Invitrogen) using random hexamers (Applied Biosystems, Foster City, CA). TaqMan assays (Applied Biosystems) were used to quantify transcripts for *Klf9* and the housekeeping gene glyceraldehyde-3-phosphate dehydrogenase (GAPDH). For *Klf9* we designed a custom TaqMan assay to span the exon/exon boundary (*Klf9* has two exons and a single intron; supplemental Table 1, published as supplemental data on The Endocrine Society's Journals Online web site at http://endo.endojournals.org). The mouse *hr* and *GAPDH* assays were purchased from Applied Biosystems. A relative quantification method (see Refs. 20 and 21) was used to compare gene expression levels by generating standard curves for each gene with a pool of cDNAs. *Klf9* and *hr* mRNA expression were normalized to *GAPDH* mRNA, which did not vary significantly across developmental stages or among treatments.

Sequence analysis and plasmid constructs

We searched for putative T_3RE half-sites in the mouse *Klf9* gene encompassing 10 kb upstream of the transcription start site, the two exons, and single intron using several online computer programs including MatInspector (version 7.7.3.1, Matrix library version 8.0; Genomatix Software GmbH, Munich, Germany), TFSEARCH version 1.3 (searches the TFMATRIX transcription factor binding site profile database by E. Wingender, R. Knueppel, P. Dietze, H. Karas; GBF-Braunschweig, Braunschweig, Germany) and PROMO using version 8.3 of TRANSFAC (22, 23). We also used the sequence analysis program Vector NTI Suite version 10 (Invitrogen) to conduct user-defined searches. Putative T_3RE half-sites identified in this manner were examined for neighboring half-sites consistent with DR-4, inverted palindrome (IP), or palindrome configurations (24). After identifying potential T_3REs, we next used a comparative genomic approach to further score DNA sequences for functional analysis. Portions of the mouse *Klf9* genomic region were aligned with rat and human genome sequences using CLUSTALW analysis in the Vector NTI Suite AlignX module (version 10; Invitrogen). Only those sequences that were conserved with rat or human or both (>50% identity) were considered for further analysis.

Oligonucleotides for native and mutant sequences based on the putative T_3REs were synthesized for use in EMSA or for generating plasmid constructs for transfection assay (see below; supplemental Table 2). For tests of the functionality of putative T_3RE sequences, constructs were generated using the pGL3 promoter plasmid (Promega, Inc., Madison, WI). Oligonucleotide duplexes were directionally cloned into the *Kpn*I and *Nhe*I sites of pGL3promoter to generate pGL3-*Klf9*[DR-4T_3RE] (corresponding to the DR-4 T_3RE located at ~3.8 kb upstream of the transcription start site; see Table 1) and pGL3-*Klf9*[DR-4T_3REmt] (a mutated DR-4 T_3RE located ~3.8 kb upstream of the transcription start site; see supplemental Table 2). The ptkDR-4Luc plasmid contains the rat growth hormone T_3RE and was a gift of Ronald Koenig (University of Michigan, Ann Arbor, MI).

EMSA

We conducted EMSA as described by Hoopfer *et al.* (12) with recombinant TRα, TRβ, and retinoid X receptor (RXR)-α produced *in vitro* using the TnT SP6 quick-coupled translation system (Promega) following the manufacturer's instructions. The ability of the wild-type or mutant m*Klf9*[DR-4 T_3RE] to displace TRβ-RXR binding to the [^{32}P]m*Klf9*[DR-4 T_3RE] probe was tested by competitive EMSA.

Cell culture and transfection assay

We used the mouse neuroblastoma cell line Neuro-2a that was engineered to express TRβ1 [N2a (TRβ1); 17] to investigate gene expression and TR association and chromatin modifications at putative T_3REs in the mouse genome. This cell line was previously shown to up-regulate *Klf9* mRNA after T_3 treatment (13). Cells were plated at a density of 0.5×10^6 cells/well in six-well plates for gene expression analyses, 1×10^5 cells/well in 24-well plates for transfection assays, or 2.5×10^6 in 100-mm tissue culture dishes for ChIP assays and cultured overnight before transfections or hormone treatments. Cells were cultured at 37 C in an atmosphere of 5% CO2–95% air in 50:50 DMEM-Hams F12 containing 500 μg/ml hygromycin B, penicillin G sodium (100 U/ml), streptomycin sulfate (100 μg/ml), and 10% thyroid hormone-stripped (25) fetal bovine serum (Invitrogen). For gene expression analyses in N2a[TRβ1] cells, the growth medium was changed to serum-free DMEM-F12 and cells were treated with T_3 for 6 h before harvest and RNA isolation.

For luciferase reporter assay experiments, we transfected cells with enhancer-reporter plasmids (200 ng DNA per well) using the FuGene 6 transfection reagent (Roche, Indianapolis, IN) following the manufacturer's instructions. All cells were cotransfected with the p*Renilla*-luciferase plasmid (10 ng/well; Promega) for normalization of cell transfection by dual-reporter luciferase assay following the manufacturer's instructions (Promega). Immediately before transfection the cells were washed twice with serum-free DMEM-F12. After 1 h the transfection medium was replaced with growth medium and the cells were incubated overnight. Cells were then treated with or without T_3 for different times before harvest and analysis of luciferase activity. Luciferase activity was quantified (measured as relative light units) using a luminometer (Femtomater FB 12; Zylux Corp., Maryville, TN). Each transfection experiment was conducted four times with three to six wells per treatment.

ChIP assay

We conducted ChIP assays on chromatin extracted from tissue culture cells and mouse brain following methods described previously with slight modifications (26, 27). We used the ChIP assay kit (Upstate Biotechnology, Inc., Lake Placid, NY) following the manufacturer's instructions. To cross-link nuclear proteins, cells or brain lysates were treated with the homobifunctional cross-linking agent dithiobis[succinimidyl propionate] (DSP; Pierce Chemical Co., Rockford, IL) (28). Cells in 100-mm dishes were washed with Dulbecco's PBS [DPBS (pH 7.4); Invitrogen], 10 ml of DPBS were added, and a 2.5-mM solution of DSP

TABLE 1. Comparison of several DR-4 T_3REs with the predicted mouse, human, and rat KLF9 DR-4 T_3REs

Sequence	Species/gene	Genomic position[a]
→ →		
AGGTCAnntaAGGTCA	Optimal DR-4 T_3RE	
AGGTGAagtgAGGTCA	mKLF9 DR-4 T_3RE	−3830 to −3804[b]
AGATTGtctgAGGTTA	hKLF9 DR-4 T_3RE	−2891 to −2875[b]
AGGTGGggcgAGGTCA	rKLF9 DR-4 T_3RE	−3837 to 3819[b]
← →		
TGACCTtgaaAGGTCA	mIntronic IP-T_3RE	+5159 to +5175[b]
→ →		
AGGTCAnntaAGGTCA	Optimal DR-4 T_3RE	
AGTTCAtctaAGGACA	xKLF9 DR-4 T_3RE	∼−6500[c]
AGGGCAtctgAGGACA	r*hr* DR-4 T_3RE	−2599 to −2584[d]
AGGCCTtctcAGGTCA	rPCP-2 DR-4 T_3RE A1	−295 to −268[e]
AGGGCAggtcAGGGAA	rPCP-2 DR-4 T_3RE A2	+207 to +227[e]
GGATTAaatgAGGTAA	hRC3/neurogranin DR-4 T_3RE	+3000 (first intron)[f]

The t nucleotides located in the third position of the spacer region are *underlined* to highlight that this position is conserved in many but not all DR-4 T_3REs. m, Mouse; x, frog (*X. laevis*); h, human; r, rat.

[a] Number of base positions upstream (−) or downstream (+) of the transcription start sites.

[b] This study. The rat and human T_3REs are located in genomic regions homologous to the region of the mouse T_3RE described in this study.

[c] (18).

[d] This DR-4 T_3RE was reported by Thompson and Bottcher (37) to be at about −9kb in the rat *hr* gene. Engelhard and Christiano (39) later localized this sequence to −2599 to −2584 upstream of the mRNA cap site. This putative DR-4 T_3RE is 100% conserved with human (39) and mouse (located −1921 to −1906; this study). The *hr* DR-4 T_3RE region analyzed in our study is that reported by Engelhard and Christiano (39), who demonstrated its functionality using transfection assays.

[e] (40).

[f] (41).

dissolved in dimethyl sulfoxide was added dropwise to a final concentration of 0.2 mM. The cells were incubated for 15 min at room temperature, the medium removed, and the cells washed with DPBS before proceeding to formaldehyde cross-linking. For the mouse brain, 0.3–0.5 mg of tissue was homogenized using a Dounce homogenizer in 0.75 ml nuclei extraction buffer [0.5% Triton X-100, 10 mM Tris-HCl, (pH 7.5), 3 mM $CaCl_2$, 0.25 M sucrose, 1 mM dithiothreitol, 0.2 mM phenylmethylsulfonyl fluoride, and 1× protease inhibitor cocktail; Sigma-Aldrich]. The stock DSP solution was added dropwise to a final concentration of 0.2 mM, and the samples were incubated at room temperature with rotation for 20 min. The samples were centrifuged at 2000 × *g* at 4 C for 2 min and the pellets washed with DPBS and resuspended in 1 ml nuclei extraction buffer. Twenty-five microliters of 37% formaldehyde were added to cross-link proteins to DNA.

The chromatin extraction procedure and DNA shearing by sonication were optimized for N2a[TRβ1] cells and mouse brain tissue. For DNA shearing by sonication, we used a sonic dismembrator 100 (Fisher, Fair Lawn, NJ). N2a[TRβ1] cells were harvested from 100-mm dishes and the cell lysates were sonicated for five cycles of 10 sec each at an output rating of 5–6 watts. For mouse brain tissue lysates, we used 10 cycles of 10 sec each at an output rating of 5–6 watts. Cell and tissue lysates were maintained on ice during the sonication procedure.

For ChIP assay we used a rabbit polyclonal antiserum raised against the full-length *Xenopus laevis* TRβ (PB antiserum provided by Yun-Bo Shi; National Institute of Child Health and Development, National Institutes of Health, Bethesda, MD). This antiserum has been used extensively for ChIP assay on frog tissues (*e.g.* Refs. 26, 29, 30), and the frog and mouse TR proteins share greater than 90% sequence identity. This antiserum does not distinguish TRα from TRβ. For acetylated histones 3 (acH3) and 4 (acH4), we used polyclonal antisera (Upstate Biotechnology; α-acH3, catalog no. 06-599; α-acH4 cat. no. 06-598; Upstate Biotechnology). To determine nonspecific binding (NSB), we either used straight normal rabbit serum (NRS; Sigma-Aldrich; for experiments with the PB antiserum) or we purified the IgG from NRS using a protein A column following the manufacturer's instructions (Pierce; for acetylated histones). The degree of enrichment in the ChIP assay for anti-TR relative to the NRS varied, depending on the treatment ($\pm T_3$) and the genomic region analyzed and ranged from about 1.5- to 7-fold. For anti-acH3 or anti-acH4, the degree of enrichment ranged from about 30- to greater than 350-fold. Negative controls for the ChIP assays included the omission of primary antibody (which uniformly produced no signal; data not shown), replacement of the primary antibody with NRS (straight or purified IgG), and the analysis of regions outside of the predicted T_3RE regions (the proximal *Klf9* promoter, the medial intron at 11.5 kb downstream of the transcription start site). ChIP samples were analyzed by real-time quantitative PCR using TaqMan assays (supplemental Table 2). Standard curves were constructed using a pool of input samples, and each ChIP sample was normalized to its respective input.

Data analysis and statistics

Data were analyzed by one-way ANOVA or *t* test using the SYSTAT computer program (version 10; SPSS Inc., Chicago, IL). Data were $\log_{10}$ transformed if the variance was found to be heterogeneous by Bartlett's test. Percentages are shown in the figures; percentages were arcsine transformed before statistical analysis. $P < 0.05$ was accepted as statistically significant. Gene expression data are reported as the mean ± SEM.

Results

Klf9 mRNA exhibits a postnatal rise in expression in mouse brain and is induced by thyroid hormone

Quantitative real-time RT-PCR analysis showed that *Klf9* mRNA in the mouse hippocampal region and cerebellum began to rise between postnatal d 4 and 7 and reached a peak at d 14 that was maintained through d 30 [Fig. 1A; hippocampus: $F_{(4, 19)} = 10.447$, $P < 0.0001$; cerebellum: $F_{(4, 19)} = 17.286$, $P < 0.0001$; one way ANOVA]. A similar pattern of gene expression was observed with *hr* mRNA [Fig. 1B; hippocampus: $F_{(4,17)} = 7.923$, $P = 0.002$; cerebellum: $F_{(4, 19)} = 32.805$, $P < 0.0001$; cerebellum

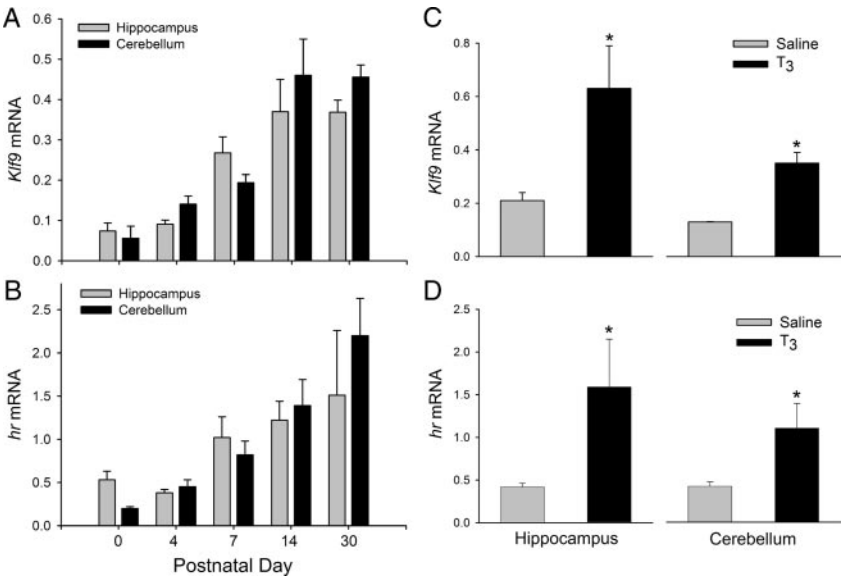

FIG. 1. Expression of *Klf9* (A) and *hr* (B) mRNAs in mouse hippocampus and cerebellum during neonatal and postnatal life (n = 3–5 per time point). Thyroid hormone induced *Klf9* (C) and *hr* (D) mRNA expression in P4 mouse hippocampus and cerebellum. Animals were given ip injections of saline (n = 6) or T_3 (25 μg/kg body weight; n = 3) and killed 4 h later. Gene expression was analyzed by quantitative real-time RT-PCR using TaqMan assays. *, Significant differences ($P < 0.05$) determined by Student's unpaired *t* test.

hr mRNA expression was elevated at P4]. Intraperitoneal injection of T_3 in P4 mice increased *Klf9* and *hr* mRNAs in hippocampus and cerebellum (Fig. 1C; *Klf9*-hippocampus: $P = 0.002$; cerebellum: $P = 0.001$; Fig. 1D; *hr*-hippocampus: $P = 0.007$; cerebellum: $P = 0.006$; *t* test).

The mouse *Klf9* gene has a DR-4 T_3RE about 3.8 kb upstream of the transcription start site

We identified a near optimal DR-4 T_3RE at 3.8 kb upstream of the predicted transcription start site of the mouse *Klf9* gene by computer analysis. The sequence of this T_3RE, and comparison with other known and predicted T_3REs are shown in Table 1, and its relative position in the mouse *Klf9* locus is shown in Fig. 2A. MatInspector (Genomatix Software) identified this T_3RE with a matrix similarity score of 0.971; a score of 1.0 is a perfect score, whereas 0.8 is considered a good score. This was the only T_3RE identified by this program within the 5′ flanking region of the gene. The other search programs that we used also identified this site. Putative DR-4 T_3REs are also present in the rat and human *Klf9* genes in homologous locations of their respective genomes (200 bp segment encompassing the T_3RE: rat, 84% identity; human, 70% identity; Table 1). For comparison, 5 kb of the 5′ flanking regions upstream of the transcription start sites of the rat and human *Klf9* genes share 75 and 70% sequence identity, respectively, with the mouse gene. The proximal promoters (500 bp) of the rat and human *Klf9* genes share 97 and 85%, respectively, with the mouse gene. We located a potential inverted palindrome T_3RE with half-sites spaced by four nucleotides (IP-4) in the mouse *Klf9* intron at +5.2 kb. This genomic region (200 bp encompassing the putative T_3RE) is conserved in the rat (91%) and human (82%) genes. For comparison, the entire introns of the rat and human *Klf9* genes share 84 and 59% sequence identity, respectively, with the mouse gene.

EMSA showed that TR-RXR heterodimers bound to the mouse *Klf9* T_3RE (Fig. 2, B and C). The binding of both TRα-RXRα and TRβ-RXRα heterodimers was reversible and of high affinity; TR monomers or homodimers did not bind. Binding of the protein complexes to the *Xenopus* TRβ T_3RE (xT_3RE) is shown for comparison to the left on the gel in Fig. 2B. Competitive binding assays with the native mouse *Klf9* T_3RE showed a DNA binding affinity in the low nanomolar range (~5 nM), whereas a mutated m*Klf9* T_3RE (see supplemental Table 2) did not displace the radiolabeled probe (Fig. 2C). TRβ-RXR heterodimers also bound to the upstream rat and human DR-4 T_3REs and the mouse intronic IP-4T_3RE (Fig. 2D).

The *Klf9* DR-4 T_3RE supports T_3-dependent transactivation

We tested for functionality of the mouse *Klf9* DR-4 T_3RE by transfection assay using putative T_3RE sequences subcloned into a minimal promoter reporter plasmid (pGL3promoter). The pGL3m*Klf9*[DR-4T_3RE] plasmid transfected into N2a[TRβ1] cells was activated by T_3 in a time-dependent manner, with increased luciferase expression at 6 h and maximum expression at 24 h [4.6-fold; Fig. 3A; $F_{(3,\ 21)} = 58.575$, $P < 0.0001$, ANOVA]. The ptkDR-4Luc plasmid included as a positive control was similarly activated by T_3 [first significant elevation at 3 h, maximum activation at 24 h, 7.2-fold; $F_{(3,21)} = 45.105$, $P < 0.0001$]; luciferase activity in cells transfected with empty vector (pGL3promoter) was not altered by T_3 treatment (data not shown).

In contrast to the native *Klf9* DR-4T_3RE, cells transfected with a plasmid containing the mutated mouse *Klf9* DR-4T_3RE (pGL3m*Klf9*[mtDR-4T_3RE]) did not show activation of luciferase expression by T_3 treatment (for 24 h; Fig. 3B; pGL3m*Klf9*[DR-4T_3RE] 5.2-fold activation, $P < 0.0001$, *t* test; ptkDR-4Luc 8-fold activation, $P < 0.0001$). Cells transfected with the plasmid containing the mutant T_3RE had a higher basal level of luciferase expression, which likely reflects the removal of the repressor activity of the unliganded TR (which represses basal activity of pGL3m*Klf9*[DR-4T_3RE] in the absence of T_3). The putative mouse intronic IP-4T_3RE and rat DR-4T_3RE were also activated by T_3, although to a lesser extent than the mouse DR-4T_3RE (~2-fold; pGL3m*Klf9*intronicIP-4T_3RE: control, 10.90 ± 0.54; T_3, 25.73 ± 1.81, $P < 0.001$, *t* test; pGL3r*Klf9*DR-4T_3RE: control, 4.58 ± 0.67, T_3, 8.45 ± 0.27, $P < 0.0001$); we did not test the putative human DR-4 T_3RE in transfection assay.

TRs associate with the *Klf9* DR-4 T_3RE region in N2a[TRβ1] cells as analyzed by ChIP assay

Treatment of N2a[TRβ1] cells with T_3 caused a dose-dependent increase in *Klf9* and *hr* mRNA levels (see supplemental

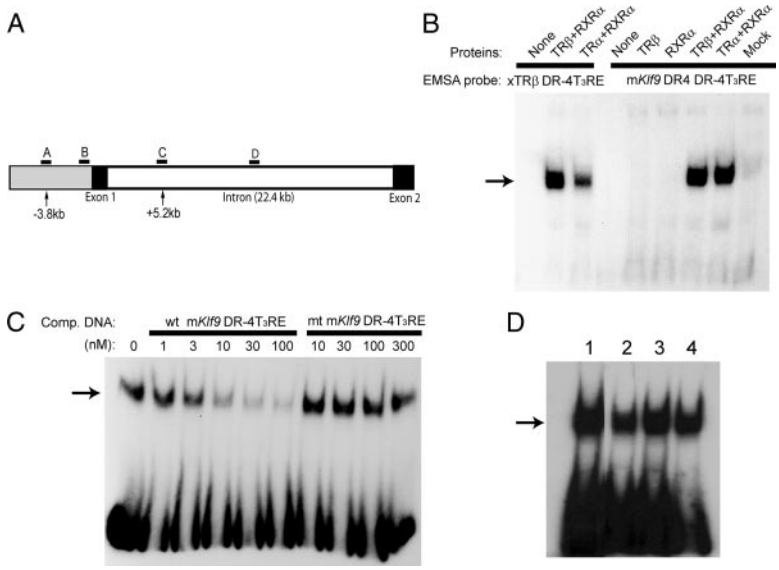

FIG. 2. TR-RXR heterodimers bind to the mouse *Klf9* DR-4 T_3RE with high affinity *in vitro*. A, Schematic representation of the mouse *Klf9* genetic locus with locations of regions targeted in the ChIP assays. The *gray shaded area* is the 5′ flanking region of the gene. *Arrows* point to the two putative T_3RE elements and indicate their positions relative to the transcription start site. *Letters* indicate the relative locations of TaqMan assays for ChIP analysis: A, upstream DR-4 T_3RE; B, proximal promoter; C, proximal intron (location of putative IP-4T_3RE); D, medial intron. B, EMSA showing that TRα-RXRα or TRβ-RXRα heterodimers bound to [^{32}P]-labeled probes derived from the mouse *Klf9* DR-4T_3RE (*right*) or the *X. laevis* TRβA promoter DR-4T_3RE (*left*; included as a positive control). TRβ or RXRα alone did not bind to either of the T_3REs. The TR and RXR proteins were produced by *in vitro* coupled transcription-translation, and 2 μl of each reaction were added to the EMSA reactions before separation by PAGE and autoradiography (see *Materials and Methods*). C, Competitive binding EMSA shows that TRβ-RXRα heterodimer binding to the mouse *Klf9* DR-4 T_3RE is displaceable and of high affinity (~5 nM). Either wild-type (wt) or mutant (mt) *Klf9* DR-4T_3RE competitor DNAs were added to EMSA reactions at different concentrations before PAGE fractionation and autoradiography. D, TRβ-RXRα heterodimers bind to the mouse *Klf9* DR-4T_3RE (lane 1), human *Klf9* DR-4T_3RE (lane 2), rat *Klf9* DR-4T_3RE (lane 3), and mouse *Klf9* intronic IP-4T_3RE (lane 4) *in vitro*. Each of the T_3RE oligonucleotides were radiolabeled with [^{32}P] and incubated with TRβ plus RXRα before PAGE fractionation and autoradiography. Each of the experiments was repeated two to three times with similar results.

Fig. 1). ChIP assays conducted on chromatin isolated from N2a[TRβ1] cells treated with T_3 for 24 h showed significant association of TRs with the mouse *Klf9* DR-4T_3RE (Fig. 4A). The TR ChIP signal was significantly different from the NRS control at the DR-4 T_3RE in untreated ($P = 0.033$; *t* test) and T_3-treated cells ($P < 0.0001$) but not at other regions of the *Klf9* gene that included the proximal promoter, the putative intronic IP-4T_3RE (~5.2 kb downstream from the transcription start site; see Table 1 and Fig. 2A) or the medial intron (11.5 kb downstream from the transcription start site). The TR ChIP signal normalized for background (TR antibody signal minus NRS signal) was significantly greater at the DR-4 T_3RE compared with other *Klf9* gene regions in both untreated and T_3-treated cells [$F_{(7,39)} = 17.851$, $P < 0.0001$; ANOVA]. We also analyzed TR association with the *hr* DR-4 T_3RE and found significant TR ChIP signal compared with NRS controls in both untreated ($P = 0.030$; *t* test) and T_3-treated ($P = 0.004$) cells. Treatment with T_3 for 24 h significantly increased TR association with the *Klf9* DR-4 T_3RE ($P = 0.008$; TR ChIP signal normalized for background); although there was a trend toward greater TR association at the *hr* DR-4T_3RE on T_3 treatment this was not statistically significant.

Thyroid hormone treatment of N2a[TRβ1] cells increases acetylation of histones 3 and 4 at the *Klf9* DR-4 T_3RE

Basal levels of acetylation of histones 3 and 4 were comparable across genomic regions analyzed (Fig. 4, B and C). Treatment of N2a[TRβ1] cells with T_3 increased acetylated histone 3 [$F_{(7, 46)} = 23.078$, $P < 0.0001$; ANOVA] and histone 4 [$F_{(7, 46)} = 30.166$, $P < 0.0001$] ChIP signals at several *Klf9* genomic regions with the largest increase at the DR-4 T_3RE (acH3, 3.3-fold; acH4, 5.9-fold). There was no significant change in either AcH3 or acH4 at the proximal promoter region. Similar increases were observed at the *hr* DR-4 T_3RE region (acH3, 2.7-fold; acH4, 3.3-fold; $P < 0.0001$ for both; *t* test).

TR associates with the *Klf9* DR-4 T_3RE in neonatal mouse brain *in vivo*

We observed a significant TR ChIP signal when compared with NRS controls at the *Klf9* DR-4 T_3RE in both hippocampus (NRS = 0.07%, TR = 0.17%, $P = 0.008$; *t* test) and cerebellum ($P = 0.01$; Fig. 5A) of neonatal mice. No significant TR ChIP signal was observed at the proximal promoter, proximal intron, or medial intron (only cerebellum analyzed). By contrast, we did not detect TR ChIP signal at the *hr* DR-4T_3RE (data not shown).

We found significant acH4 ChIP signal compared with NRS controls at each region of the mouse *Klf9* gene except at the medial intron in hippocampus and cerebellum ($P < 0.05$; *t* tests; Fig. 5, B and C; only acH4 was analyzed due to limitation in the amount of available chromatin). There were significant differences in normalized acH4 ChIP signal across the *Klf9* gene in both hippocampus [$F_{(3,15)} = 4.361$, $P = 0.027$] and cerebellum [$F_{(3, 15)} = 4.167$, $P = 0.031$] with the highest signal at the *Klf9* DR-4 T_3RE. A similar high level of acH4 signal was observed at the *hr* DR-4 T_3RE in both brain regions (acH4 *vs.* NRS: hippocampus, $P = 0.01$; cerebellum, $P = 0.029$; *t* test).

Discussion

We identified a T_3RE of the DR-4 type at 3.8 kb upstream of the transcription start site of the mouse *Klf9* gene to explain its regulation by thyroid hormone. TR-RXR heterodimers bound to the mouse DR-4 T_3RE with high affinity *in vitro*, and the sequence supported T_3-dependent transactivation in transfection assays. Furthermore, ChIP assays showed that TRs associated with this T_3RE in the mouse-derived cell line N2a[TRβ1] and neonatal mouse brain *in vivo*, and treatment with T_3 led to hyperacetylation of histones at this site. We also provide further evidence that the DR-4 T_3RE discovered in mammalian *hr* genes [at ~2 kb upstream of the transcription start site in mouse, ~2.6 kb in rat and human; Engelhard and Christiano (39)] is a *bona fide* hormone response element.

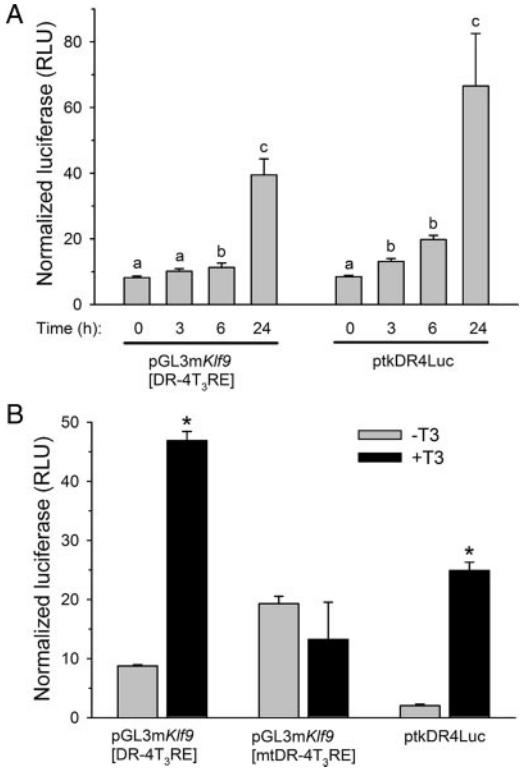

FIG. 3. The mouse *Klf9* DR-4 T_3RE confers thyroid hormone responsiveness to a minimal, heterologous promoter. A, Treatment with T_3 (30 nM) increases luciferase activity in cells pGL3m*Klf9*[DR-4T_3RE] in a time-dependent manner. N2a[TRβ1] cells were transiently transfected with pGL3m*Klf9*[DR-4T_3RE] or ptkDR-4Luc (rat GH T_3RE; positive control) and treated with T_3 for the times indicated before harvest and analysis of cell lysates by dual-luciferase assay. *Letters* indicate significant differences among means ($P < 0.05$; Fisher's least squares difference test). B, Mutation of the mouse *Klf9* DR-4T_3RE eliminates T_3-dependent transactivation in transfection assay. N2a[TRβ1] cells were transiently transfected with pGL3m*Klf9*[DR-4T_3RE], pGL3m*Klf9*[mtDR-4T_3RE] (mutated T_3RE) or ptkDR-4Luc and treated with T_3 (30 nM) for 24 h. Luciferase activity in cells transfected with empty vector (pGL3promoter) was not altered by T_3 treatment (data not shown). *, Statistically significant differences ($P < 0.05$; Student's unpaired *t* test). The data shown in the graphs are the mean ± SEM of the relative light units (RLU) of firefly luciferase divided by the RLU for the Renilla luciferase. Each transfection experiment was conducted four times with three to six wells per treatment.

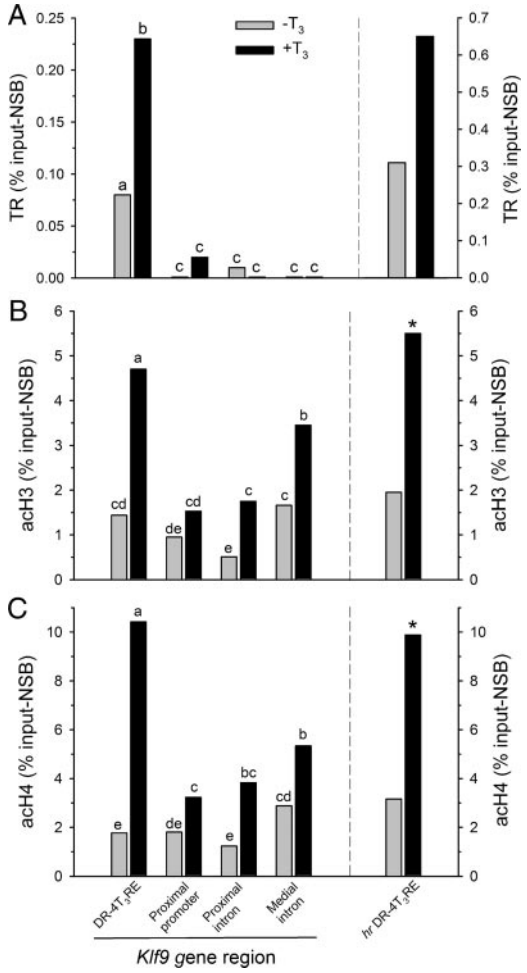

FIG. 4. A, TR associates with the mouse *Klf9* DR-4T_3RE and the *hr* DR-4T_3RE in N2a[TRβ1] cells as analyzed by ChIP assay. N2a[TRβ1] cells were treated with or without T_3 (30 nM) for 24 h before harvest for ChIP assay. ChIP samples were analyzed by real-time quantitative PCR using TaqMan assays that targeted the genomic regions indicated (and see supplemental Table 2). The TR ChIP signals at the *Klf9* DR-4T_3RE and the *hr* DR-4 T_3RE were significantly increased by T_3 treatment. Treatment with thyroid hormone causes hyper-acH3 (B) and -acH4 (C) in N2a[TRβ1] cells as analyzed by ChIP assay. NSB was assessed by ChIP using NRS (A) or IgG purified from NRS (B and C). Shown are the mean ChIP signals expressed as a percentage of the input minus the NSB. Statistical analyses were conducted on *arcsine* transformed data, and *letters* indicate significant differences among means ($P < 0.05$; Fisher's least squares difference test; n = 6/treatment). *, Statistically significant differences ($P < 0.05$; Student's unpaired *t* test; n = 6/treatment).

Krüppel-like factor 9 promotes differentiation of mammalian and amphibian neuronal cells, mediating T_3 actions on neurite extension and branching (13–15). Disruption of the *Klf9* gene in mouse led to behavioral abnormalities characteristic of defects in the hippocampus, cerebellum, and amygdala and reduced dendritic arborization of cerebellar Purkinje cells (16). The *Klf9* gene was isolated as a direct T_3 response gene in the frog (11, 31), and we showed that rat *Klf9* is also regulated by T_3 and exhibits a rise in expression in the brain beginning in the neonatal period (13). Similar to our findings in rat brain, here we report that mouse *Klf9* is developmentally regulated, with postnatal expression in both the hippocampus and cerebellum increasing up to 30 d of age, paralleling the postnatal rise in plasma T_3 (1). Injection of T_3 into P4 mice elevated *Klf9* mRNA in the hippocampus and cerebellum, which supports our findings in the rat that the postnatal rise in *Klf9* expression is dependent on thyroid hormone (13).

The rapid kinetics of *Klf9* up-regulation by T_3 in N2a[TRβ1] cells, the fact that T_3 induction of *Klf9* mRNA is resistant to protein synthesis inhibition, and the fact that nuclear run-on assay showed that T_3 initiates *Klf9* transcription (13) suggested that mouse *Klf9* is a direct T_3 response gene. Furlow and Kanamori (18) provided evidence for a DR-4 T_3RE located about 6.5 kb upstream of the transcription start site of the frog *Klf9* gene. We therefore searched for T_3REs in the mouse *Klf9* gene to explain its regulation by T_3. TRs bind to DNA at the consensus hexamer sequence (G/A)GGT(C/G)A, referred to as a half-site because TRs function predominantly as dimers. Most known T_3REs are comprised of two half-sites that are arrayed as either direct repeats spaced by four nucleotides (DR-4), IPs spaced by four to six nucleotides or palindromes (Pal) (reviewed in Ref. 24). TRs can bind to T_3REs as monomers or homodimers, but the preferred configuration is a heterodimer with RXR (24),

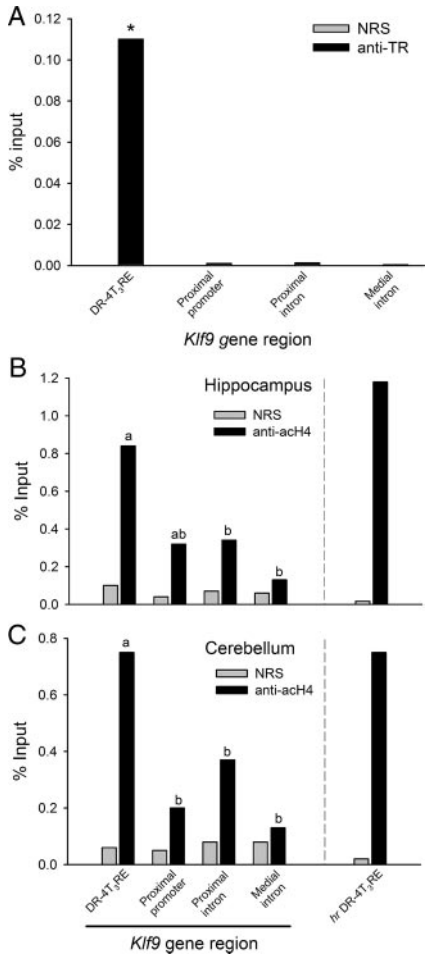

FIG. 5. A, TR associates with the mouse *Klf9* DR-4 T_3RE in neonatal mouse cerebellum as analyzed by ChIP assay. P4 mice were injected with T_3 (25 μg/kg body weight) and brain tissue harvested 4 h later for chromatin extraction and ChIP assay (see *Materials and Methods*). acH4 is elevated at the *Klf9* DR-4 T_3RE and the *hr* DR-4 T_3RE in mouse hippocampus (B) and cerebellum (C) as analyzed by ChIP assay. ChIP samples were analyzed by real-time quantitative PCR using TaqMan assays that targeted the genomic regions indicated in the graph (and supplemental see Table 2). Shown in the graphs are the mean ChIP signals expressed as a percentage of the input for PB anti-TR serum (anti-TR) or NRS. However, statistics were conducted on the normalized TR or acH4 ChIP values, *i.e.* the mean ChIP signals expressed as a percentage of the input minus the NSB. NSB was assessed by ChIP using NRS (A) or IgG purified from NRS (B and C) For anti-TR, the ChIP signal was significantly greater than for NRS only at the DR-4 T_3RE (*, $P < 0.05$; Student's unpaired *t* test; n = 4). For anti-acH4, the ChIP signal was significantly greater than for NRS IgG at all regions of the *Klf9* gene except the medial intron; statistics shown in the graphs do not compare the mean anti-acH4 *vs.* NRS ChIP signals but instead the normalized anti-acH4 ChIP values among *Klf9* gene regions (*letters* indicate significant differences among means; $P < 0.05$; Fisher's least squares difference test; n = 4). Anti-acH4, Purified IgG to acetylated histone 4.

as we also found in our gel shift assays using the mouse *Klf9* DR-4T_3RE (see Fig. 2). TR-RXR heterodimers exhibit a strong preference for DR-4, and DR-4T_3REs are the most common and best-characterized response elements (24). Studies in the frog *X. laevis* using ChIP assay confirmed that TR-RXR is associated with DR-4 elements in the TRβ and basic leucine zippertranscription factor (TH/bZip) gene promoters *in vivo* during tadpole metamorphosis (26).

Using computer analysis, we identified putative T_3REs upstream and within the mouse *Klf9* gene. We chose for analysis two sequences based in part on the strong conservation of the genomic regions in which they were found among mouse, rat, and human, one at −3.8 kb and one within the intron at about +5.2 kb. The −3.8 kb T_3RE is of the type DR-4 with head-to-tail orientation of half-sites, whereas the intronic T_3RE has the configuration of an inverted palindrome with half-sites spaced by four nucleotides (IP-4). Other putative T_3REs found in the upstream region or intron by computer analysis were represented by single half-sites [T_3REs of almost all positively regulated genes are comprised of two or more half-sites; (24)], poor matches to known T_3REs, or were not conserved across species and thus were not studied further. We cannot rule out the possibility that other functional T_3REs not identified by this approach that may influence *Klf9* gene expression are present within, near, or far upstream or downstream of the *Klf9* locus, and further study is required to test this.

We found that both putative mouse *Klf9* T_3REs were bound by TR-RXR heterodimers in gel shift assays and that both supported T_3-dependent transactivation in transfection assay. However, whereas TR was found to be associated with the −3.8 kb DR-4 T_3RE in both N2a[TRβ1] cells and mouse brain *in vivo* by ChIP assay, we found no association of TR with the putative intronic IP-4 T_3RE region, thus failing to support that this sequence is a functional T_3RE. This finding illustrates that, although a putative T_3RE may be bound by TR-RXR *in vitro* and may support T_3-dependent transcription in transfection assay, analysis of TR association with the genomic region *in vivo* by ChIP assay is necessary to test whether the element is functional. Treatment of N2a[TRβ1] cells with T_3 increased the ChIP signal at both the *Klf9* and *hr* upstream DR-4 T_3RE regions but not at the proximal promoter, proximal intron, or medial intron of the *Klf9* gene. The increased TR signal at the upstream *Klf9* DR-4 T_3RE (and the *hr* DR-4T_3RE) further supports that this region possesses a *bona fide* hormone response element. In the unliganded state, TRs are associated with chromatin and are not thought to be recruited to genomic sites on hormone binding as occurs for some other members of the steroid receptor superfamily (32). By contrast, we found evidence for recruitment of TRs to T_3REs upon hormone binding. Because the expression of TRβ1 in N2a[TRβ1] cells is maintained at a constant level through stable transfection (17) and we previously showed that T_3-dependent *Klf9* expression is mediated by TRβ1 and not TRα1, it is unlikely that the increased TR ChIP signal was due to increased TR biosynthesis. Buchholz *et al.* (30) reported that TR association with the *Xenopus* TRβ and basic leucine zipper transcription factor (TH/bZip) promoters *in vivo* was increased by treatment of tadpoles with T_3. This increase could have been due to T_3-dependent recruitment of TRs to genomic sites or perhaps as a result of increased TR biosynthesis, which occurs in tadpoles [TRβ autoinduction; (33)]. Our findings suggest that whereas TR associates with T_3REs in the genome in the unliganded form, additional TR recruitment to T_3REs may occur on ligand binding *in vivo*. An alternate explanation is that ligand binding to TR or histone modifications at the T_3RE caused by T_3-dependent recruitment of coregulators to this site may expose epitopes on TR, thus resulting in more efficient ChIP. Further study is required to distinguish these potential mechanisms.

The TR-RXR heterocomplex recruits coregulator proteins that mediate the repressive or activational actions of the complex by recruiting histone modifying enzymes such as histone acetyltransferases and histone deacetylases, among others (34, 35). We observed robust increases in the acetylation of histones 3 and 4 at the upstream *Klf9* DR-4T_3RE caused by T_3 treatment in N2a[TRβ1] cells and significantly greater acH4 at the DR-4T_3RE compared with other regions of the *Klf9* gene in mouse brain *in vivo*. The level of histone acetylation was greatest at the upstream DR-4T_3RE, but elevated histone acetylation caused by T_3 treatment was observed at all regions of the *Klf9* locus analyzed. The widespread histone acetylation could be due to spreading of histone modifications across the genetic locus originating from the site of TR binding. Interestingly, histone acetylation at the proximal *Klf9* promoter was the least affected by T_3. Parker *et al.* (36) recently reported in *Drosophila* cells that, on activation of Wnt signaling, acetylation of histones 3 and 4 spread over relatively large genomic regions occupied by the Wnt target genes *naked cuticle* and *Notum,* with relatively small changes occurring at the promoter regions of these genes. By contrast, histone acetylation was restricted to the promoter regions of housekeeping genes that were not activated by Wnt. Whether such spread of histone acetylation, with the hormone response element acting as a nucleation site, is a characteristic of hormone-responsive genes requires further study.

The *hr* gene encodes a zinc-finger domain transcription factor that interacts with TRs and function as a corepressor (37, 38). The *hr* mRNA exhibited developmental stage and T_3-dependent regulation in mouse brain similar to that of *Klf9*. Also, we found TR association and T_3-dependent histone acetylation with the predicted *hr* DR-4T_3RE located at about −2 kb. Although we found TR association with the *hr* DR-4T_3RE in N2a[TRβ1] cells, we were unable to confirm this in mouse brain *in vivo*. Thus, our evidence supports that the mouse *hr* gene has a functional T_3RE at about 2 kb upstream of the transcription start site, but further study is required to elucidate its role in mouse brain *in vivo*.

Taken together, our findings support the presence of a functional DR-4 T_3RE at 3.8 kb upstream of the transcription start site of the mouse *Klf9* gene to explain its regulation by T_3 during early postnatal life. We also provide evidence that this T_3RE may be evolutionarily conserved among mammals. We found that TRs may be recruited to chromatin on ligand binding, and future studies should analyze dynamic changes in TR recruitment, corepressor/coactivator exchange, and histone modifications at the mouse *Klf9* gene and other T_3-responsive genes *in vivo*.

Acknowledgments

We are grateful to Yun-Bo Shi for providing the PB antiserum and Anna Ray and Jifei Geng for technical assistance. We are also grateful to Pia Bagamasbad for conducting the quantitative RT-PCR analyses for *hr* mRNA. Ron Koenig kindly provided the ptkDR-4Luc and the TR and RXR expression plasmids. Jack Puymirat provided the N2a[TRβ1] cells.

Address all correspondence and requests for reprints to: Dr. Robert J. Denver, Department of Molecular, Cellular, and Developmental Biology, The University of Michigan, Ann Arbor, Michigan 48109-1048. E-mail: rdenver@umich.edu.

This work was supported by National Institutes of Health Grant 1R01NS046690-01 (to R.J.D.).

Disclosure Summary: The authors have nothing to disclose.

References

1. **Porterfield SP, Hendrich CE** 1993 The role of thyroid hormones in prenatal and neonatal neurological development—current perspectives. Endocr Rev 14: 94–106
2. **Bernal J** 2002 Action of thyroid hormone in brain. J Endocrinol Invest 25: 268–288
3. **Legrand J** 1982 [Thyroid hormones and maturation of the nervous system]. J Physiol (Paris) 78:603–652 (French)
4. **McEwen BS, Coirini H, Danielsson A, Frankfurt M, Gould E, Mendelson S, Schumacher M, Segarra A, Woolley C** 1991 Steroid and thyroid hormones modulate a changing brain. J Steroid Biochem Mol Biol 40:1–14
5. **Gould E, Allan MD, McEwen BS** 1990 Dendritic spine density of adult hippocampal pyramidal cells is sensitive to thyroid hormone. Brain Res 525:327–329
6. **Gould E, Woolley CS, McEwen BS** 1991 The hippocampal formation-morphological changes induced by thyroid, gonadal and adrenal hormones. Psychoneuroendocrinology 16:67–84
7. **Gould E, Westlind-Danielsson A, Frankfurt M, McEwen BS** 1990 Sex differences and thyroid hormone sensitivity of hippocampal pyramidal cells. J Neurosci 10:996–1003
8. **Imataka H, Sogawa K, Yasumoto K, Kikuchi Y, Sasano K, Kobayashi A, Hayami M, Fujii-Kuriyama Y** 1992 Two regulatory proteins that bind to the basic transcription element (BTE), a GC box sequence in the promoter of the rat P-4501A1 gene. EMBO J 11:3663–3671
9. **Kaczynski J, Cook T, Urrutia R** 2003 Sp1- and Kruppel-like transcription factors. Genome Biol 4:206
10. **Suske G, Bruford E, Philipsen S** 2005 Mammalian SP/KLF transcription factors: bring in the family. Genomics 85:551–556
11. **Denver RJ, Pavgi S, Shi YB** 1997 Thyroid hormone-dependent gene expression program for *Xenopus* neural development. J Biol Chem 272:8179–8188
12. **Hoopfer ED, Huang L, Denver RJ** 2002 Basic transcription element binding protein is a thyroid hormone-regulated transcription factor expressed during metamorphosis in *Xenopus laevis*. Dev Growth Differ 44:365–381
13. **Denver RJ, Ouellet L, Furling D, Kobayashi A, Fujii-Kuriyama Y, Puymirat J** 1999 Basic transcription element binding protein (BTEB) is a thyroid hormone-regulated gene in the developing central nervous system: evidence for a role in neurite outgrowth. J Biol Chem 274:23128–23134
14. **Cayrou C, Denver RJ, Puymirat J** 2002 Suppression of the basic transcription element-binding protein in brain neuronal cultures inhibits thyroid hormone-induced neurite branching. Endocrinology 143:2242–2249
15. **Bonett RM, Hu F, Bagamasbad P, Denver RJ** 2009 Stressor and glucocorticoid-dependent induction of the immediate early gene Krüppel-like factor 9: implications for neural development and plasticity. Endocrinology 150:1757–1765
16. **Morita M, Kobayashi A, Yamashita T, Shimanuki T, Nakajima O, Takahashi S, Ikegami S, Inokuchi K, Yamashita K, Yamamoto M, Fujii-Kuriyama Y** 2003 Functional analysis of basic transcription element binding protein by gene targeting technology. Mol Cell Biol 23:2489–2500
17. **Lebel JM, Dussault JH, Puymirat J** 1994 Overexpression of the β-1 thyroid receptor induces differentiation in Neuro-2a cells. Proc Natl Acad Sci USA 91:2644–2648
18. **Furlow JD, Kanamori A** 2002 The transcription factor basic transcription element-binding protein 1 is a direct thyroid hormone response gene in the frog *Xenopus laevis*. Endocrinology 143:3295–3305
19. **Bagamasbad P, Howdeshell KL, Sachs LM, Demeneix BA, Denver RJ** 2008 A role for basic transcription element-binding protein 1 (BTEB1) in the autoinduction of thyroid hormone receptor β. J Biol Chem 283:2275–2285
20. **Crespi EJ, Denver RJ** 2006 Leptin (*ob* gene) of the South African clawed frog *Xenopus laevis*. Proc Natl Acad Sci USA 103:10092–10097 (article featured in NSF Discoveries)
21. **Yao M, Stenzel-Poore M, Denver RJ** 2007 Structural and functional conservation of vertebrate corticotropin-releasing factor genes: evidence for a critical role for a conserved cyclic AMP response element. Endocrinology 148:2518–2531
22. **Farré D, Roset R, Huerta M, Adsuara JE, Roselló L, Albà MM, Messeguer X**

2003 Identification of patterns in biological sequences at the ALGGEN server: PROMO and MALGEN. Nucleic Acids Res 31:3651–3653
23. **Messeguer X, Escudero R, Farré D, Núñez O, Martínez J, Albà MM** 2002 PROMO: detection of known transcription regulatory elements using species-tailored searches. Bioinformatics 18:333–334
24. **Yen PM** 2001 Physiological and molecular basis of thyroid hormone action. Physiol Rev 81:1097–1142
25. **Samuels HH, Stanley F, Casanova J** 1979 Depletion of L-3,5,3′-triiodothyronine and L-thyroxine in euthyroid calf serum for use in cell-culture studies of thyroid hormone. Endocrinology 105:80–85
26. **Sachs LM, Shi YB** 2000 Targeted chromatin binding and histone acetylation *in vivo* by thyroid hormone receptor during amphibian development. Proc Natl Acad Sci USA 97:13138–13143
27. **Buchholz DR, Paul BD, Shi Y-B** 2006 Chromatin immunoprecipitation for *in vivo* studies of transcriptional regulation during development. In: Whitman M, Sater AK, eds. Analysis of growth factor signaling in embryos. Boca Raton, FL: CRC Press; 257–271
28. **Nowak DE, Tian B, Brasier AR** 2005 Two-step cross-linking method for identification of Nf-κB gene network by chromatin immunoprecipitation. Biotechniques 39:715–725
29. **Sachs LM, Jones PL, Havis E, Rouse N, Demeneix BA, Shi YB** 2002 Nuclear receptor corepressor recruitment by unliganded thyroid hormone receptor in gene repression during *Xenopus laevis* development. Mol Cell Biol 22:8527–8538
30. **Buchholz DR, Paul BD, Shi YB** 2005 Gene-specific changes in promoter occupancy by thyroid hormone receptor during frog metamorphosis: implications for developmental gene regulation. J Biol Chem 280:41222–41228
31. **Brown DD, Wang Z, Furlow JD, Kanamori A, Schwartzman RA, Remo BF, Pinder A** 1996 The thyroid hormone-induced tail resorption program during *Xenopus laevis* metamorphosis. Proc Natl Acad Sci USA 93:1924–1929
32. **Mangelsdorf DJ, Thummel C, Beato M, Herrlich P, Schütz G, Umesono K, Blumberg B, Kastner P, Mark M, Chambon P, Evans RM** 1995 The nuclear receptor superfamily. The second decade. Cell 83:835–839
33. **Tata JR** 2000 Autoinduction of nuclear hormone receptors during metamorphosis and its significance. Insect Biochem Mol Biol 30:645–651
34. **Wu Y, Koenig RJ** 2000 Gene regulation by thyroid hormone. Trends Endocrinol Metab 11:207–211
35. **McKenna NJ, O'Malley BW** 2002 Combinatorial control of gene expression by nuclear receptors and coregulators. Cell 108:465–474
36. **Parker DS, Ni YY, Chang JL, Li J, Cadigan KM** 2008 Wingless signaling induces widespread chromatin remodeling of target loci. Mol Cell Biol 28:1815–1828
37. **Thompson CC, Bottcher MC** 1997 The product of a thyroid hormone-responsive gene interacts with thyroid hormone receptors. Proc Natl Acad Sci USA 94:8527–8532
38. **Potter GB, Beaudoin 3rd GM, DeRenzo CL, Zarach JM, Chen SH, Thompson CC** 2001 The hairless gene mutated in congenital hair loss disorders encodes a novel nuclear receptor corepressor. Genes Dev 15:2687–2701
39. **Engelhard A, Christiano AM** 2004 The hairless promoter is differentially regulated by thyroid hormone in keratinocytes and neuroblastoma cells. Exp Dermatol 13:257–264
40. **Zou L, Hagen SG, Strait KA, Oppenheimer JH** 1994 Identification of thyroid hormone response elements in rodent Pcp-2, a developmentally regulated gene of cerebellar Purkinje cells. J Biol Chem 269:13346–13352
41. **Martínez de Arrieta C, Morte B, Coloma A, Bernal J** 1999 The human RC3 gene homolog, NRGN contains a thyroid hormone-responsive element located in the first intron. Endocrinology 140:335–343